

## Improving shallow water multibeam target detection at low grazing angles

Douglas Luiz da Silva Pereira<sup>1,2</sup> and John E. Hughes Clarke<sup>1</sup>

1. Ocean Mapping Group (OMG), Department of Geodesy and Geomatics Engineering,  
University of New Brunswick (UNB), Canada

2. Directorate of Hydrography and Navigation (DHN), Brazilian Navy

### ABSTRACT

Beyond  $\sim 60^\circ$  incidence angle, many modern multibeam echo sounders have difficulty maintaining sufficient depth accuracy and seabed target detection to comply with International Hydrographic Organization (IHO) standards. In some cases, a target at such a low grazing angle is not detected due to limitations of the existing bottom detection method and filters applied by the manufacturer. In lieu of clear positive bathymetric indicators, a data gap within the bathymetric surface or a shadow in the backscatter image may be the only indication of the presence of that target.

This paper presents a refined bottom detection algorithm based on the Bearing Direction Indicator (BDI) method. The algorithm can be applied in post processing as long as the water column data is retained. This approach can markedly improve target detection capability at low grazing angles in shallow waters by independently discriminating each echo's direction of arrival irrespective of the beam spacing. Two test datasets were collected using an EM 2040D employing angular sectors as wide as  $\pm 82^\circ$ . Data were acquired over a site with multiple IHO compliant anthropogenic objects to assess the ability to detect low grazing angle targets prior to, and after, application of the newly-developed algorithm. Results obtained clearly illustrate that the BDI algorithm can enhance low grazing angle target detection capability.

### 1. INTRODUCTION

Multibeam Echo Sounders (MBES), in comparison with Single Beam Echo Sounders (SBES), provide larger seafloor coverage due to the use of multiple beams distributed over an angular sector oriented transversally to the ship. This capability allows MBES users to ensonify the bottom at incidence angles away from just the nadir direction. However, the data quality from the inner beams, including both accuracy and resolution, is generally significantly better than those from the outer beams.

Most single head MBES have an angular coverage of around  $130^\circ$ . Dual head ones, in contrast, can potentially cover the whole sector ( $180^\circ$ ) underneath the ship. Even with dual receivers, however, for the purpose of seabed mapping, usable angular coverage is mainly limited due to sound wave attenuation, refraction and weak low grazing angle backscattering. In shallow waters (less than 40 m), sectors of up to around  $160^\circ$  to  $170^\circ$  are possible. Nevertheless, beyond approximately  $120^\circ$ , both depth accuracy and target detection capability degrade rapidly.

Imperfect compensation for refraction is the main factor degrading depth accuracy in the outer beams. Beams close to horizontal are more susceptible to errors in depth measurement,

especially in an environment with rapidly varying sound velocity structure. In this case, many successive layers (with their own uncertainties) associated with high beam incidence angle leads to greater depth errors. Also, particularly roll sensor errors have a great contribution to the depth accuracy degradation away from nadir. Small roll errors are disproportionately detrimental to the outer beam data. Nevertheless, in stable water masses and with proper integration, IHO depth accuracy can usually be maintained beyond  $60^\circ$ . Beyond that point, however, the target detection becomes the limiting factor.

IHO requirements for target detection are order-dependent (IHO special publication S-44, 2008). Table 1 presents the standards.

Table 1: Target detection standards (after IHO special publication S-44, 2008)

	Survey Order			
	Special	1a	1b	2
Minimum size of features to be detected	1-meter cube	2-meters cube up to 40 meters depth; 10% of depth beyond 40 meters	Not required	Not required

Previous experiments have shown that IHO level multibeam target detection in shallow waters is successfully achieved until approximately  $60^\circ$  of incidence angle in most modern MBES (Hughes Clarke *et al.*, 2013). Beyond that point, detection capability usually degrades. Many factors individually or in combination are responsible for this difficulty. The bottom-projected beam footprint, which is dependent on the beamwidth, depth and grazing angle, is one of the major controls on the spatial resolution and therefore affects the system's ability to resolve small targets. The greater the beamwidth, depth and incidence angle, the larger the projected beam footprint. Targets at the size of, or smaller than, the beam footprint may not be adequately resolved. To work inside the dimension of that footprint requires bottom detection algorithms that do not utilize the full beam echo time series. Most modern systems now typically provide outer swath solution density much tighter than the projected physical beamwidth. It is not clear, however, whether such density is always justified.

Other factors that limit outer swath detection include the widening effect of beams steered away from broadside to the receiver, which augments the loss in spatial resolution. The across and along-track sounding densities derived from the beam spacing and the combination of vessel speed, ping rate and yaw stabilization capability, respectively, limit the feature detection capacity as well.

In addition to geometric aspects, even when the system embodies the required angular resolution to resolve small targets out of  $60^\circ$  of incidence angle, limitations of the built-in bottom detection algorithms and applied filters may mask them, making it difficult to distinguish one within its surrounding area. In most of the cases, a target-derived shadow in the backscatter image is the only indication that some object is located where shadow begins (Fig. 1).

In order to cover more ground and therefore to reduce survey time, the Brazilian Navy (lead author's sponsor) intends to purchase a contemporary dual head MBES, manufacturer Kongsberg<sup>®</sup>, model EM 2040D to be applied in the shallow waters of Amazon River and Paraguay River Basins. The dual receiver version of the EM 2040 is particularly adapted to wide

swaths as the tilted receivers maintain narrower beams at wider incidence angles. Thus, potentially wider swath angular sectors could be employed.

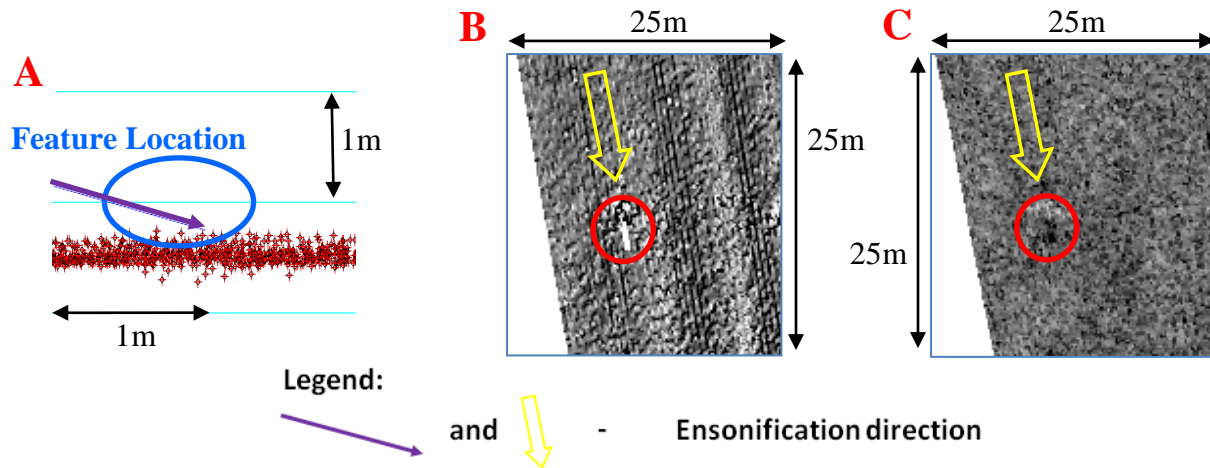


Figure 1: Example of an undetected 1-meter cube imaged with  $68^\circ$  of incidence angle at 20 meters depth (after Hughes Clarke et al., 2013)

Across-track depth profile (A), Digital Terrain Model (DTM) (B) and backscatter image (C) on the vicinity of a 1-meter cube as seen with  $68^\circ$  of incidence angle by using a MBES Kongsberg<sup>®</sup> EM 2040D (set to 300 kHz) at 20 meters depth. Note that the object may not be considered detected. Data gap on DTM and shadow on backscatter image (highlighted red circles) are a possible, yet not necessarily sufficient, indication of the object presence

Motivated by that future acquisition, this research project worked on the issue of some MBES not confidently detecting small targets beyond around  $60^\circ$  of incidence angle (outer beams) in shallow waters. The project focus is on developing an enriched non-conventional bottom detection algorithm. The developed algorithm, based on the Bearing Direction Indicator (BDI) bottom detection method, markedly enhances targets “visibility” at low grazing angles, thus improving target detection capability.

This paper is structured in five sections. The current section introduced the problem being addressed and the approach used to minimize it. Section 2 provides the background related to this research and discussion of previous works. Section 3 presents the details and constraints of the developed algorithm. Performed tests and achieved results are discussed in section 4. Section 5 finalizes stating the conclusions of this work.

## 2. BACKGROUND

### 2.1 Review of multibeam bottom detection techniques

Three bottom detection methods are most widely used: Weighted Mean Time (WMT), Bearing Direction Indicator (BDI) and Phase Detection (both zero-phase and high definition).

WMT computation is based on the intensity time series recorded within a single receiver beam channel (de Moustier, 1993). Given the echo Direction Of Arrival (DOA) implicitly assumed to be the maximum response axis of the steered beam, the Time Of Arrival (TOA) is calculated. The goal of WMT is to determine the instant when the boresite of the transmitter beam hits the bottom. The most common approach to calculate center-beam instant is to consider it as being

the center of mass of the echo envelope (weighted mean time) over a defined threshold. This method delivers one solution per beam. WMT works well as long as the echo envelope is short as the uncertainty in the time estimation remains low. Therefore, it is primarily utilized for close-to-normal incidence.

Second bottom detection method BDI is based on the angle series at a specific Two-Way Travel Time (TWTT). BDI has the inverse approach of WMT. Given the echo TOA, DOA(s) is(are) calculated (de Moustier, 1993). Its goal is to determine the direction(s) from where acoustic intensity is maximum, which represent locations on the seabed being ensonified at the TWTT considered. As the recorded directions from where echoes are received are restricted to the discretely spaced beams axes, a curve fitting technique around the representation of the receiver main lobe beamwidth in the angle series plot is needed in order to more precisely estimate the maximum acoustic direction. In addition, unlike WMT, BDI is primarily used for oblique incidence as the bottom-projected pulse length is short as opposed to normal incidence, resulting in lower uncertainty in angle estimation. BDI calculation delivers one or more angle solutions per time slice.

The third bottom detection method is called Phase Detection (Hammerstad *et al.*, 1991). Similarly to WMT, Phase Detection also calculates the TOA, given the DOA. The calculation is based on the echo phase difference between two overlapping and offset virtual array of transducers elements arranged perpendicular to the beam axis. For each time sample within a beam, a phase difference computation is performed. When the value is zero, the signal is assumed to be coming from the beam axis and this moment is recorded as being the echo TOA. Zero-crossing Phase Detection yields one solution per beam as well.

By expanding Phase Detection method to values of phase difference other than zero, it is possible to attain more than one depth per beam (Nilsen, 2012). For instance, phase differences of  $-\pi/4$ ,  $+\pi/4$ ,  $-\pi/2$ ,  $+\pi/2$ ,  $-3\pi/4$  and  $+3\pi/4$  are values commonly used. This enhanced Phase Detection method is called High Definition Beam Forming (HDBF). Phase Detection (both zero-phase and high definition) is primarily used for oblique incidence as the phase slope is gentle under this circumstance as opposed to normal incidence. In that case, the zero or any other angle crossing is more accurately identified.

## 2.2 Discussion of previous works

Some authors recently addressed the issue of in-water object identification and tracking by exploring Water Column (WC) data. van der Werf (2010) proposed a post-acquisition method to identify the peak of any mast-like object in-between surface and bottom and afterwards translate the correspondent WC “pixel” to the geographic reference frame. Although his method is robust and extremely useful for safety of navigation purposes where least depth determination is critical, only in-water high aspect ratio (fraction of height over width) target identification was addressed. In addition, the methodology is highly dependent on well-trained hydrographers.

Videira Marques (2012) went beyond van der Werf and implemented an automatic mid-water target detection and tracking, even though no seabed-located object identification technique was approached. His method involved picking a peak in intensity in all of time, elevation angle and along-track, making use of predicted pulse length and receiver and transmitter beamwidths. In

this sense, the DOA picking is equivalent to BDI though he did not interpolate the samples in order to estimate the “real” maximum acoustic direction.

In contrast to in-water targets, it has been seen among literature investigation that so far shallow waters seabed target detection in the very outermost beams (beyond 60° of incidence angle) has been poorly explored. The issue of accuracy and resolution loss in the outer beams is well known by hydrography community. However, very few works have addressed and explored those sometimes disregarded data for seabed target detection purposes.

Specifically dealing with vertical accuracy assessment and target detection capability in shallow waters, Hughes Clarke *et al.* (2013) showed that both bathymetric tracking and feature detection in compliance with IHO Special Order standards are only reliable until 60° of beam incidence angle. In that study, they analyzed data collected by the MBES Kongsberg® EM 2040D over a site with lots of deployed unnatural targets in different sizes and shapes (Hughes Clarke, 2013). According to them, as Kongsberg® Maritime (KM) uses both WMT and Phase Detection in its MBES and knowing that the second method is the preferred and most accurate one for grazing incidence, phase disturbance is a potential indicator of target detection failure beyond around 60°. Although target-derived shadow is shown in most analyzed cases, that shadow by itself is not an unquestionable evidence of an object presence.

In fact, high aspect ratio targets, such as 1-meter cubes, may lead to a within-beam layover geometry (the common slant range problem) when illuminated at low depression angles (Fig. 2). Under these circumstances, the sound wave front hits the inboard face of the feature practically at a normal incidence and target-projected pulse length spreads out over a wide range of elevation angles. Those simultaneous echoes from the target and the seabed in front disturb the phase calculation as more than one scattering point comes into play. Subsequent to the disturbed echo, random phase in the shadow window will further invalidate the phase slope. The resultant split-beam phase difference may be a meaningless value or a very misleading one (Fig. 2). The adjustment curve through some phase difference samples around the intended boresite-relative angle will be then strongly biased by that “spike”. As the phase curve fitting is a mix of layover echoes and noise in shadow, the resulting curve-fit variance is high. Thus, normally the bottom detection is aborted (Hammerstad *et al.*, 1991; Nilsen, 2012), resulting in a characteristic sounding data gap (Fig. 1A).

In the event of a rejected Phase Detection, if WMT is used as the alternate method, multiple beams around the target report the identical slant range resulting in a false arc of solutions (Fig. 3A). The reason for that is that the relative level of the near-specular target strength, compared to the surrounding seabed, is often greater than the side lobe suppression. Earlier bottom detection implementations by KM prior to 2010 (Fig. 3B) proved exactly that result (Hughes Clarke, 2009). Subsequent tests on the same targets with a modified algorithm indicate that WMT solutions of similar slant range are now rejected leaving just a hole (Hughes Clarke, 2010). Somehow the KM current bottom detection algorithm filters out those unrealistic depths and instead no solution is delivered. As a result, only a characteristic data gap remains.

While the current KM bottom detection algorithm might not identify an outer beam target, the logged Water Column Imagery (WCI) can be used to recognize its presence (Fig. 4). The same arc of potential solutions that corrupts the WMT is indicative of the target. If an alternate

approach can be placed, then perhaps the target could be recovered. WCI data have many applications and uses (Hughes Clarke, 2006). One of them is to calculate a new bottom pick.

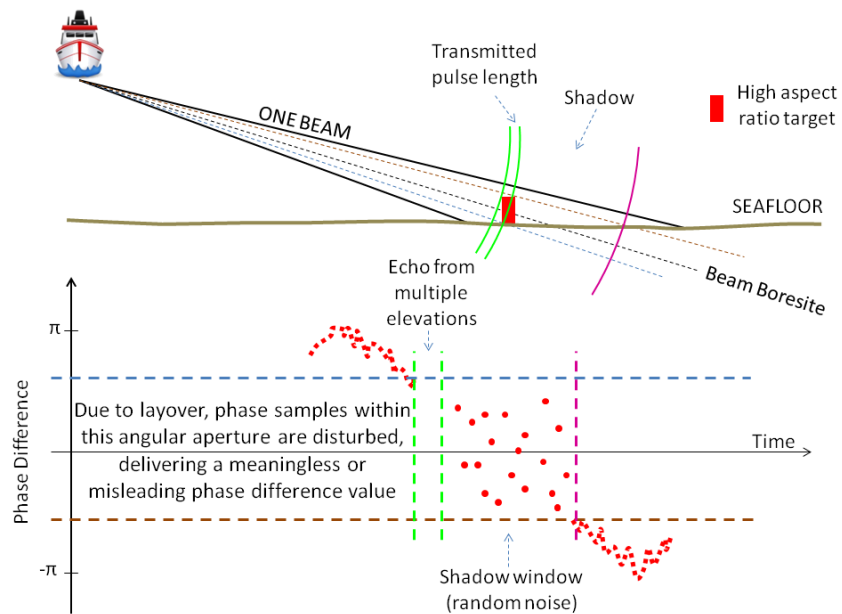


Figure 2: Within-beam common slant range phase disturbance

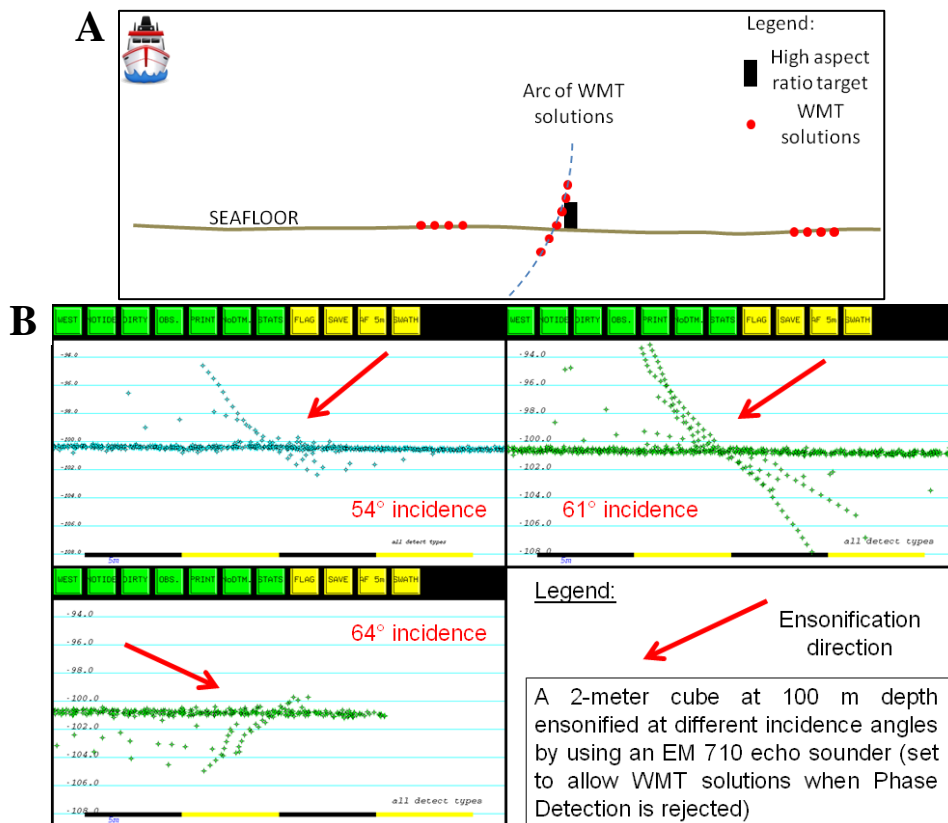


Figure 3: WMT arc of solutions when facing a high aspect ratio target (after Hughes Clarke, 2009)

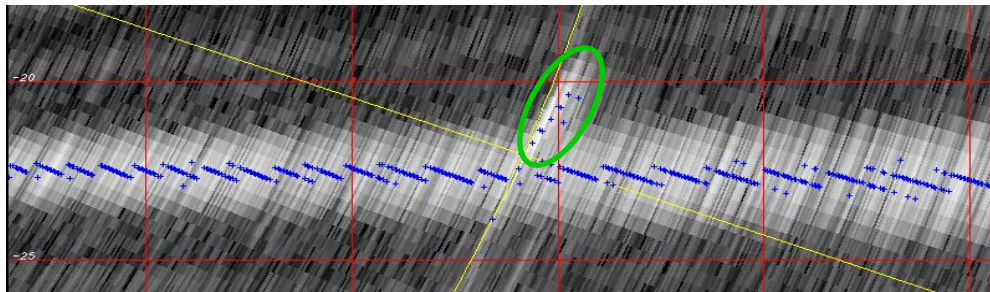


Figure 4: Across-track Water Column Image (section) highlighting the inboard edge (green ellipse) of the non-detected 1-meter cube presented on figure 1 (after Hughes Clarke *et al.*, 2013)

Small blue crosses represent the highest in-the-beam-axis-direction echo amplitudes for each time slice

In the same 2013 study, Hughes Clarke *et al.* illustrated that the BDI method (Satriano *et al.*, 1991; de Moustier, 1993) could provide such an alternate approach to the KM depth solutions as a way of improving high aspect ratio target definition. By their proposal, a composite WMT, BDI and Phase Detection technique would be bestowed altogether.

BDI method “was used at a time for a minority of MBES and looks like to be abandoned today” (Lurton, 2010). For oblique incidence, Phase Detection has generally replaced BDI as finer angular discrimination through multi-sample phase curve fitting and more accurate results are possible. This, however, is strictly only true in the absence of high aspect ratio targets. This limitation becomes more acute at incidence angles beyond  $60^\circ$ . Under that geometry, the target “appearance” in WCI data indicates that BDI is not so affected by layover and poor signal-to-noise conditions as Phase Detection is. BDI may thus potentially be utilized as an alternative method to reveal any not-previously detected abrupt seabed object.

### 3. METHODS

In order to investigate and assess the potential BDI ability to improve multibeam shallow water target definition at low grazing angles, an enriched BDI bottom detection algorithm was developed. Calculations are performed based on the recorded Water Column (WC) data. Three main resources characterize the algorithm: the echo DOA refinement, the compression or not of the final depth solutions and the possibility of selecting the detection threshold either manually (user-defined) or automatically. The two last resources allow the computation of the BDI solutions in different fashions.

#### 3.1 DOA refinement

The task of determining DOA-TOA pairs by applying the BDI technique is, in principle, straightforward. Having the WC data, the algorithm just needs to sweep all time slices (TOAs) and for each of them find the beams (DOAs) with the highest amplitudes among their close neighbors if over a defined threshold. In practice, however, this approach by itself results in solutions with angular discrimination no finer than the physical beam spacing as, within a beam, all echoes are stored into the WC data as coming from the beam axis.

In order to obtain an angular discrimination smaller than the beam spacing, a curve fitting technique around the representation of the receiver main lobe beamwidth in the angle series plot

was applied, following the approach of Satriano *et al.* (1991). The receiver beam pattern in elevation was taken into account. By refining the DOA, more than one solution per beam with its own DOAs other than the beam axis can be computed. Under these circumstances, the longer footprints of the outer beams accommodate more time slices and consequently more BDI solutions, resulting in an increased across-track sounding density and potentially better short wavelength object definition.

A specific seabed scattering target is sensed by many surrounding beams and not only by the closest beam. The receiver beam pattern in elevation is almost symmetric around its maximum response axis. Thus, in a hypothetical non-noise environment with a strong echo coming from a direction that coincides exactly with a beam axis at a certain time  $t$  and that beam's immediate neighbors having the same beam pattern, the central beam records a strong magnitude and its adjacent neighbors a lower and equal one (Fig. 5). The previous reasoning makes sense only if at time  $t$  no other echo is received by the transducer other than that one whose incoming direction coincides with the considered central beam axis and equiangular beam spacing configuration.

In case of incoming energy direction not coincident with a beam axis, prior and posterior beams store different amplitudes, the higher one associated with the closest neighbor beam (Fig. 6). Similar concept applies to other close beams other than the two immediate neighbors.

Hence, following the model of Satriano *et al.* (1991) and SeaBeam<sup>®</sup> (2000), it seems reasonable to fit a parabola in the angle series plot over the highest amplitude beam and its close neighbors to estimate the maximal amplitude direction. Having the fitting parabola equation, its peak point determines the interpolated "real" highest amplitude (ordinate) and correspondent incoming direction (abscissa), this last one being the refined echo DOA (Figs. 5 and 6).

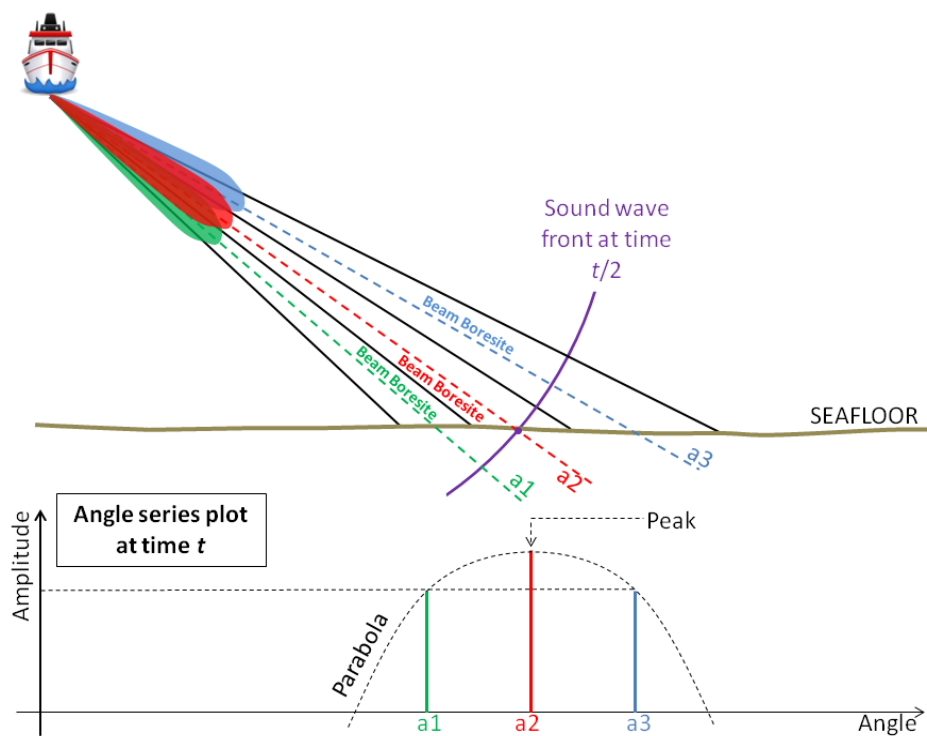


Figure 5: Angle series plot when echo direction coincides with a beam axis (3 beams illustration)

The developed BDI algorithm applies, therefore, parabola fitting for the echo DOA refinement. A parabola passing through 5 amplitude-angle pairs (the highest intensity beam and its closest 2 adjacent beams in each side) presumably associated with a detection is calculated. A Least Squares Approximation technique (Davis, 1975) considering all samples equally weighted was implemented. Based on the fitted parabola equation  $F(x) = ax^2 + bx + c$ , its vertex's abscissa  $x_v = \frac{-b}{2a}$  represents the estimated and refined seabed echo DOA.

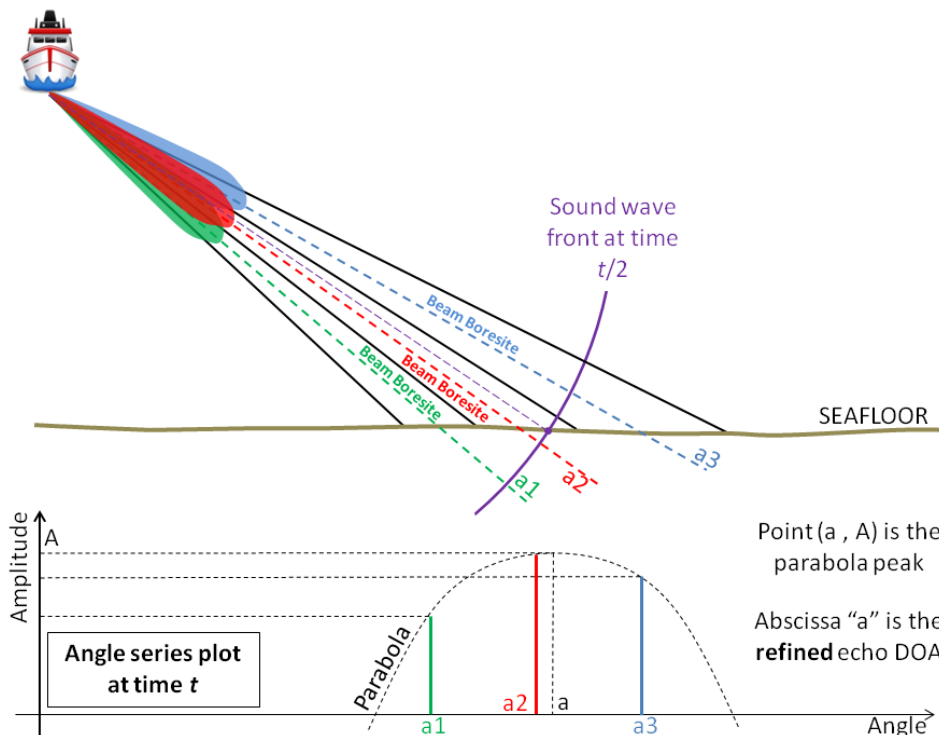


Figure 6: Angle series plot when echo direction is not coincident with a beam axis (3 beams illustration)

Fig. 7 shows an example of solutions for the same seafloor section in two different fashions: closest peak and 5-point parabola BDI.

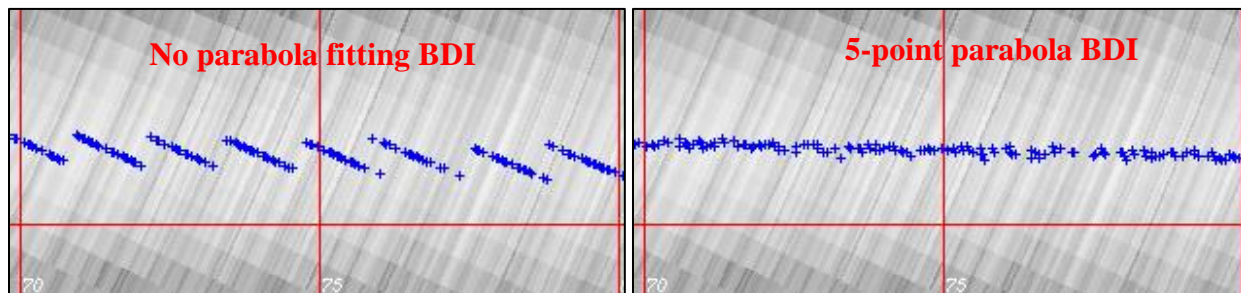


Figure 7: Closest peak versus 5-point parabola BDI

Closest peak (left) and 5-point (right) parabola BDI solutions. Notice that 5-point parabola BDI yields a smaller angular discrimination, resulting in a more representative shape of the actual seafloor topography

A parabola fitting technique for estimating the maximal amplitude direction is fundamentally an attempt to model the receiver beam pattern in elevation. The term “estimation” is well suited

because in reality, due to the electronic beam steering process applied to flat transducers (case of EM 2040D) and its consequent beamwidth fattening effect with the increase of the steering angle, each beam has its own pattern. Parabola fitting then is just an approximation as even adjacent beams have slightly different patterns as the steering is slightly distinct. In addition, noise and water column and sub-bottom backscatter strength variations across the whole angular coverage at the considered time  $t$  interfere and mix with the bottom return signal recorded by the central beam's surrounding beams. This could bias the values for each discrete beam, resulting in an apparent offset DOA. Interestingly, even if there is noise, as all beams are sampled at the same instance, as long as the noise is not strongly directional, it will overprint on all beams identically, thereby not significantly distorting the DOA.

It must be added that the viability of parabola fitting is dependent on the receiver main lobe beamwidth and the beam spacing. In order to make sense when using DOA parabola fitting as an attempt to model the shape of the receiver main lobe beamwidth, a simple relation must be met. The beam spacing must be smaller than the effective receiver main lobe beamwidth divided by the number of beams used in the fitting process (5). In other words, all 5 beams must be within the effective receiver main lobe beamwidth.

It is also important to cite that the tighter the beam spacing, the more the number of samples within the effective receiver main lobe beamwidth. Theoretically, the more the number of samples used in the parabola fitting with respect to the number of all samples within the physical beamwidth, the better the model. Also, the narrower the physical receiver beam, the more confident the angle and the less likely that layover within the beam will occur. To this end, for high incidence angles the tilted receivers of the EM 2040D are significantly superior to the horizontal single receiver of the EM 2040S.

### **3.2 Detection thresholding**

While the echo of interest is at the intended DOA, at all angles for a given TWTT, there will always be spurious noise resulting in secondary peaks. In order to avoid mistakenly picking a false detection, a minimum cut-off intensity value (detection threshold) must be set. Only samples above the detection threshold are considered. Its setting is crucial. It must be somehow adjusted to a value greater than the background noise level and the peaks of the side lobes. The main outcomes of incorrect threshold setting are loss of real solutions and appearance of undesirable (and sometimes unavoidable) outliers. The developed BDI algorithm permits the threshold setting either manually (user-defined) or automatically. The manual approach is intended for development purposes to design an optimal operational automatic threshold.

#### **3.2.1 Manual thresholding**

For the user-defined approach, the user chooses a threshold value based on the previous analysis of the extracted peaks from each time slice of the normalized data (with the TVG, Time Varying Gain, implemented). The chosen value is then applied for all time slices within the swath. The ideal threshold must clearly separate the peak echoes from the body. Fig. 8 shows a user-defined threshold example applied for a particular EM 2040S swath.

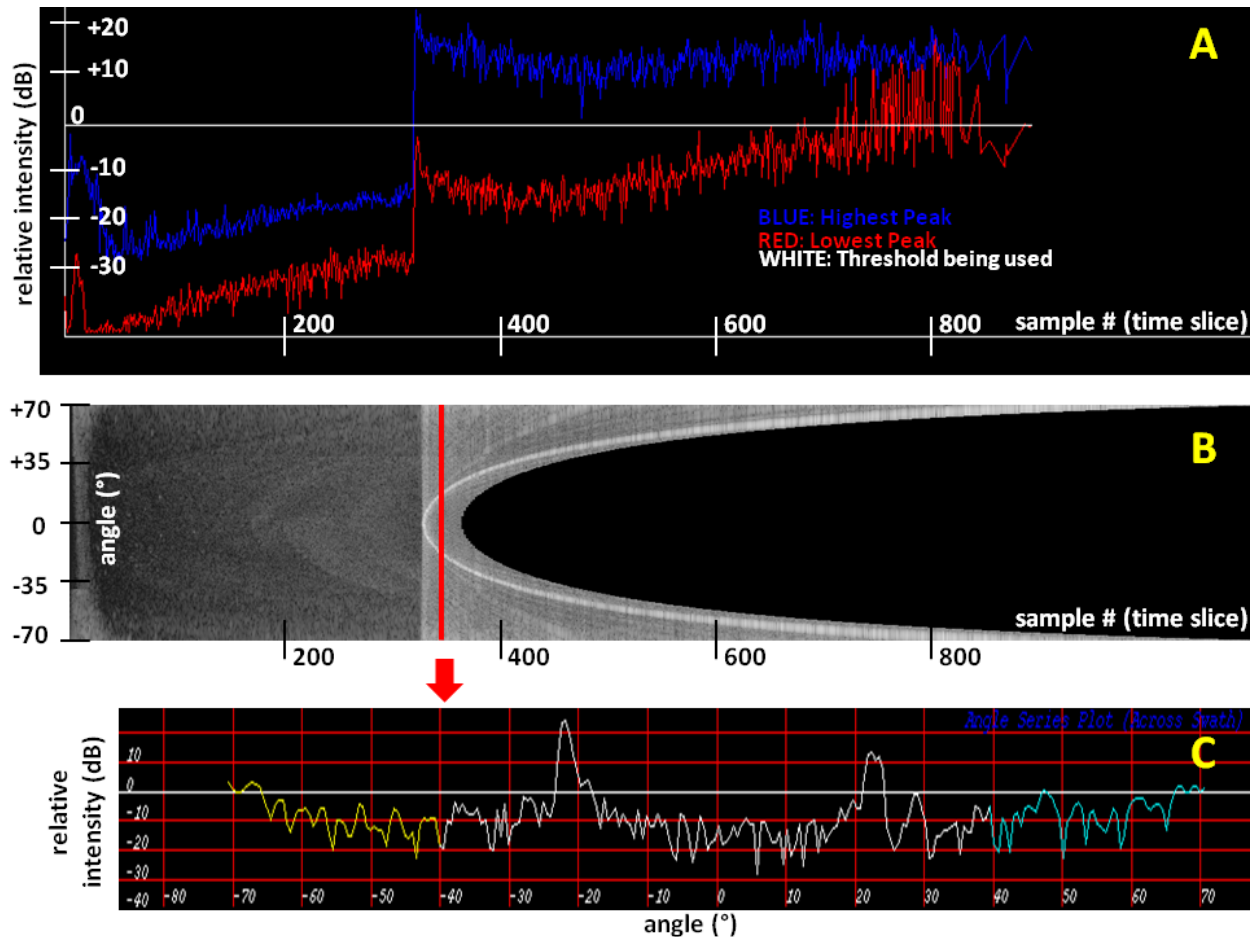


Figure 8: User-defined threshold example for a particular EM 2040S swath

A – the blue and red lines represent the highest and lowest peaks, respectively, of each time slice of the recorded WC data for that particular swath. The WC data has had a  $30\log R$  TVG applied ( $R$  is the range). The white horizontal straight line represents the manually set threshold value. In this particular example case, only peaks above that are solutions to be considered. B – the corresponding WC time-angle plot from which the highest and lowest peaks are extracted. C – the angle series plot (across swath) for the time slice highlighted in red on B. Note that the two peaks around  $-22^\circ$  and  $+23^\circ$  are the solutions to be considered in the BDI algorithm, meaning one seafloor interaction for each side of the swath.

### 3.2.2 Automatic thresholding

Normally, as the seabed backscatter level varies spatially, the threshold should be adaptive. Additionally, as the noise floor rises with time, the threshold should identify the cutoff of usable data. Similarly, when shadows occur, the threshold criteria should identify and reject these time windows. Thus, an automatic threshold algorithm must take into account all these requirements.

The automatic thresholding algorithm developed for this research calculates the “most appropriate” and unique threshold value for each time slice without input from the user. Calculation is based on the side lobes’ strengths relative to the main lobe for each normalized time slice data (e.g., Fig. 8C). The algorithm works as follows:

**1<sup>st</sup> Step:** (Fig. 9) for each time slice, identify all peaks on the angle series plot and their maximum (*max*) and minimum (*min*) values, as in Fig. 8A (blue and red lines, respectively).

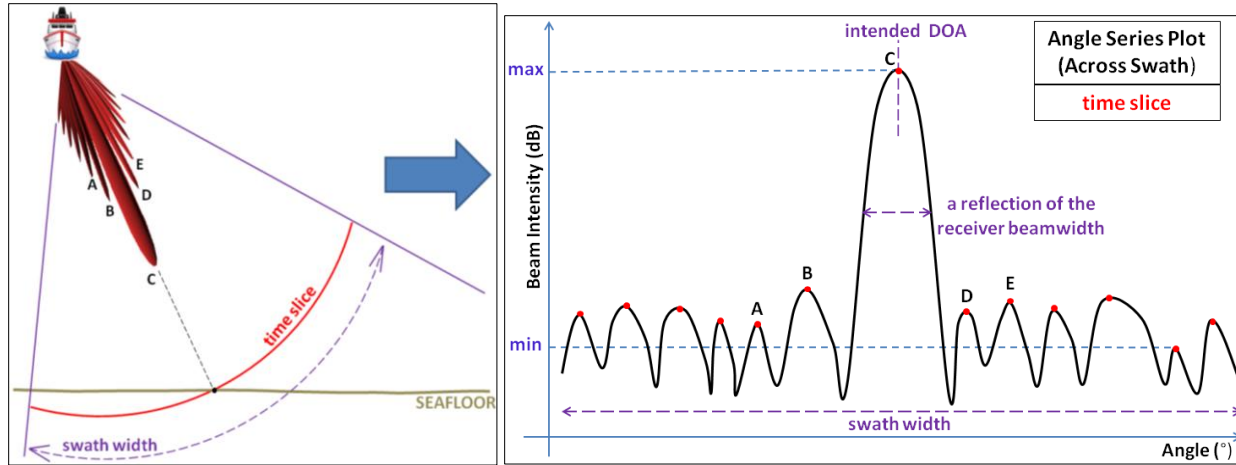


Figure 9: Automatic Threshold Algorithm – Step 1  
 Identification of all peaks (red dots on right hand image) and their maximum and minimum values

2<sup>nd</sup> Step: (Fig. 10) calculate the mean of all peaks ( $mean_{all}$ ), the mean of the maximum and minimum peaks ( $mean_{max\_min}$ ) and open up an interval of 10% of  $(max - min)$  centered on  $mean_{max\_min}$  whose limits are defined by  $[ lower_{limit} ; upper_{limit} ]$  where  $lower_{limit} = max - 0.55 * (max - min)$  and  $upper_{limit} = max - 0.45 * (max - min)$ .

3<sup>rd</sup> Step: apply the following rule to define the threshold: if  $lower_{limit} \leq mean_{all} \leq upper_{limit}$ , which means that all peaks have very similar intensities or the lack of one or more “main lobes”, then the threshold is set to a high value above which it does not expect any echo intensity. Else, which means that one or more strong peaks (“main lobes” or detections) are pushing the  $mean_{max\_min}$  upwards, then the threshold is set to:  $THRESHOLD = max - 0.15 * (max - min)$ . In the first case, for the time slice considered, no detection is found. In the second one, all distinct grouped samples above the threshold are solutions to be considered (Fig. 10).

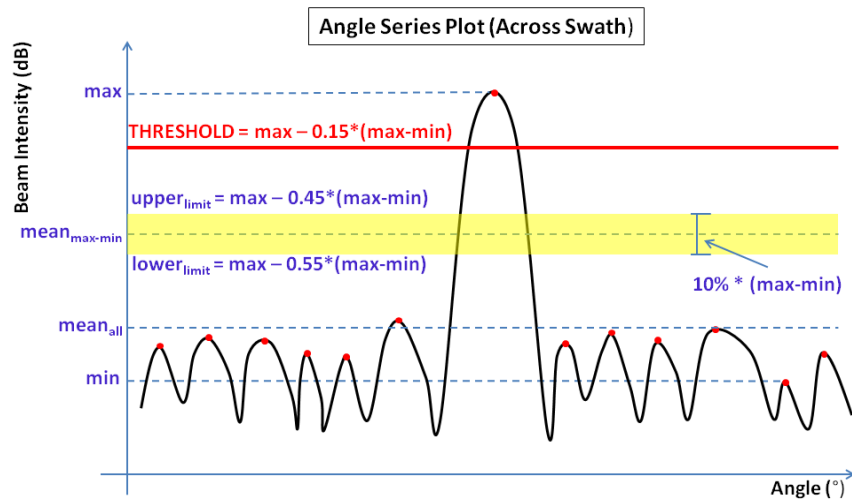


Figure 10: Automatic Threshold Algorithm – Steps 2 and 3

Calculation of  $mean_{all}$ ,  $mean_{max\_min}$ ,  $lower_{limit}$ ,  $upper_{limit}$  and threshold definition. If  $mean_{all} < lower_{limit}$  or  $mean_{all} > upper_{limit}$ ,  $THRESHOLD = max - 0.15 * (max - min)$ . Else,  $THRESHOLD = 100 \text{ dB}$

This automatic threshold technique is based on the significant difference in terms of intensity between the main and side lobes. As for each time slice only a few detections (mostly two on non-tilted receivers or one on tilted ones) are expected amidst many almost with the same strength side lobes, the mean of all peaks is slightly displaced upwards if compared with a situation with no detection. An example of a case with no detection would be in the shadow behind a target. Conversely, the mean of the maximum and minimum peaks is strongly pushed upwards when a detection is found. The proximity or not between  $mean_{all}$  and  $mean_{max\_min}$  is, therefore, the key to the threshold definition.

### 3.3 Compression

In normal mode, EM 2040D provides up to 256 depth solutions per receiver, which means a maximum one solution per physical beam forming channel. In high density mode, up to 400 solutions per receiver are provided, meaning approximately a maximum average of 1.56 solutions per physical beam, with generally more per beam at higher incidence angles.

One of the main characteristics of DOA-refined BDI is the possibility of having as many solutions as the number of time slices within the bottom interaction window for each beam. Depending on the applied amplitude threshold, the time sampling and the number of time slices within all 256 beams' bottom-projected footprints, refined BDI method might deliver more than 400 solutions per receiver. An average greater than 1.56 solutions per beam can be achieved. This augmented sounding density potentially improves short wavelength feature definition, especially for those objects ensounded by the outermost beams where the density of the BDI solutions is higher due to the smaller pulse length footprint (considering a flat seafloor). This is essentially one of the main reasons why a BDI algorithm was developed for this research. However, by sampling all time slices, some solutions may be contaminated by noise resulting in misleading representation of the actual seabed topography. Hence, it is necessary to find a balance between finer sampling and averaging to promote noise suppression.

Given that some BDI solution averaging might reduce noise on a smooth seafloor, but too much averaging could dampen out the expression of targets, what is a suitable level of sample combination on compression? What happens if the BDI solutions are compressed to deliver up to the same number of solutions provided by the manufacturer? Is the target detection capability still improved? In order to answer these questions and also to expand the range of this research, a compression algorithm was developed. It works as follows:

1<sup>st</sup> Step: (Fig. 11) a flat seafloor is assumed.

2<sup>nd</sup> Step: (Fig. 11) the width of the across-track swath, based on the angular sector, is calculated at the approximate depth of the Minimum Slant Range (MSR).

3<sup>rd</sup> Step: (Fig. 11) the full across-track swath width is divided in equally spaced (equidistant)  $n$  virtual beam footprints.  $n$  is defined by the user.

4<sup>th</sup> Step:  $n$  virtual beams are created based on the equidistant virtual beam footprints (Fig. 12). Thus, the virtual beam spacing is variable. For each virtual beam, an averaging angle is defined based on the spacing. This is referred to as the virtual beamwidth. Virtual beams close to nadir are wider. As the beams move to the outer region, the virtual beamwidth reduces gradually. The

idea is to obtain after compression a sampling of the bottom as equidistant as possible (limited by the flat seafloor assumption). Note that the averaging is performed over a range of angles significantly narrower than the physical beamwidth.

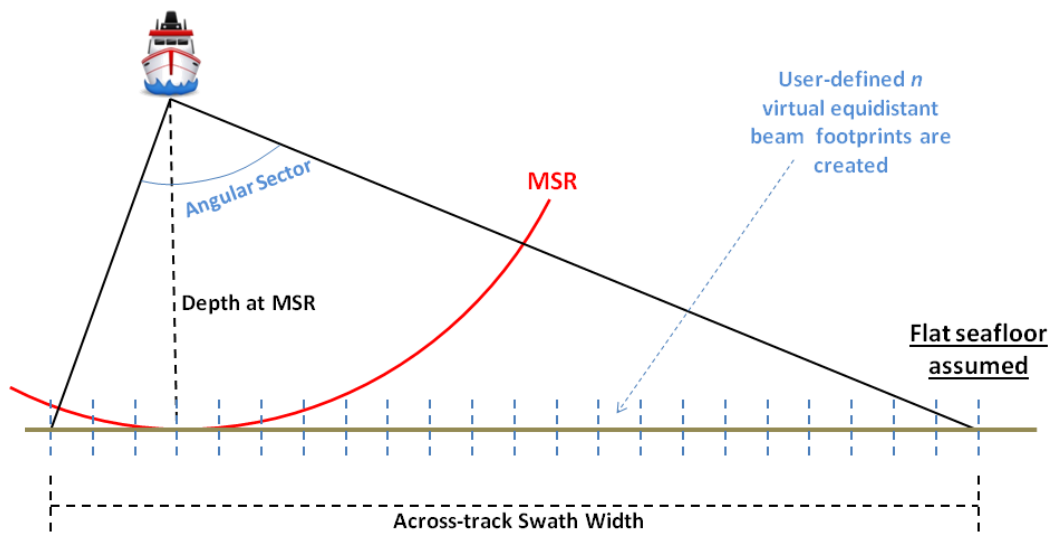


Figure 11: Illustrating 1<sup>st</sup>, 2<sup>nd</sup> and 3<sup>rd</sup> Steps of the compression algorithm

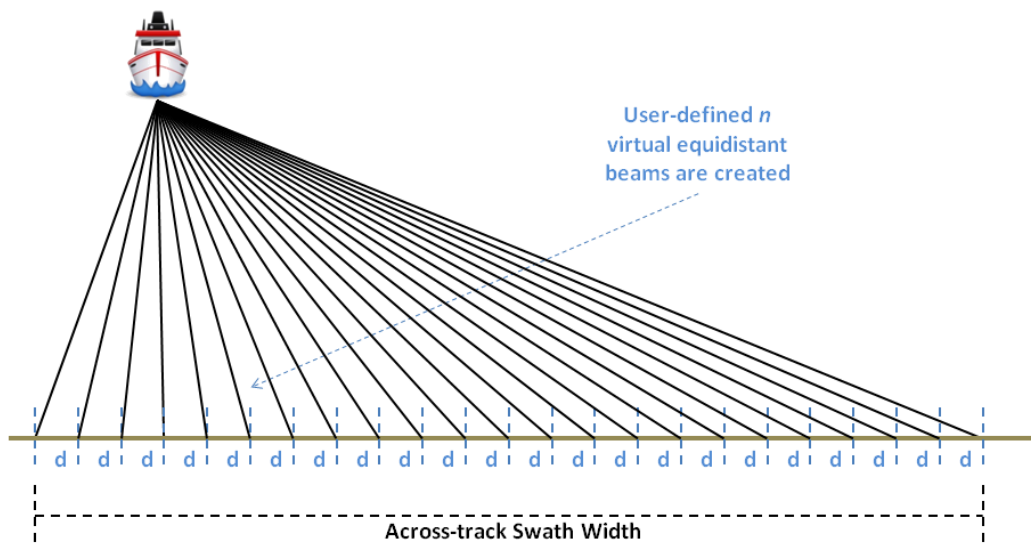


Figure 12: Illustrating the 4<sup>th</sup> Step of the compression algorithm

5<sup>th</sup> Step: for each virtual beam, two means are calculated for all BDI solutions enclosed by it: a sample-number-based mean ( $\mu_{\text{time}}$ ) and DOA-based mean ( $\mu_{\text{angle}}$ ). Both statistics are weighted by the sample intensity with respect to mean backscatter level at the TWTT considered (mean of all peaks in the angle series plot). The final compressed BDI TOA/DOA pair solution then for each beam is the calculated couple  $\mu_{\text{time}} / \mu_{\text{angle}}$  (Fig. 13). The end result is a maximum one BDI solution per virtual beam.

It must be noticed that the final angle result is not necessarily the virtual beam axis. In addition to the flat seafloor assumption, this not-in-the-virtual-beam-axis solution degrades the initial

attempt to achieve an equidistant sampling of the bottom after compression. Also, unlike the original SeaBeam® (2000) approach, the solution angular spacing is not equiangular and is significantly finer than the physical beamwidth.

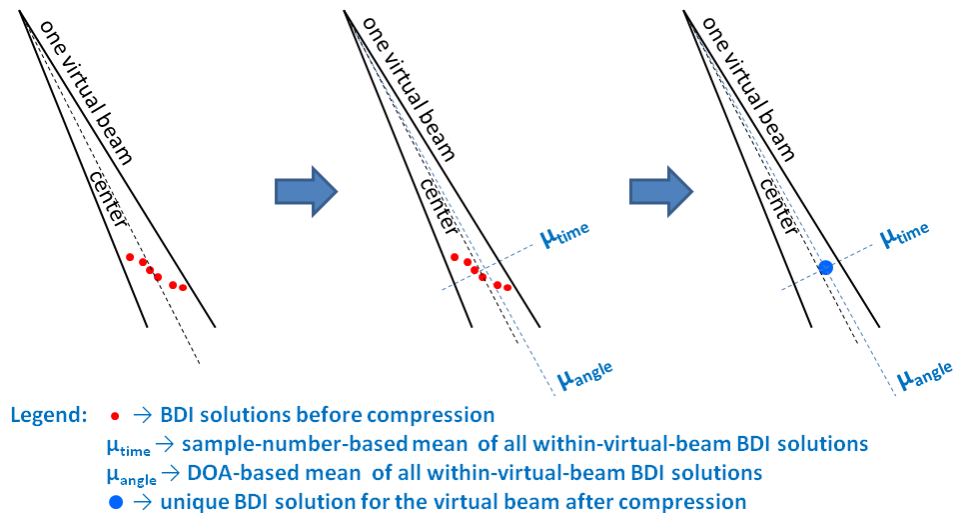


Figure 13: Illustrating the 5<sup>th</sup> Step (final) of the compression algorithm

#### 4. TESTS AND RESULTS

Two datasets were used to test the algorithm developed for this research. They consist of a series of lines of multibeam bathymetric surveys collected during the 2013 and 2014 summers jointly by the United States Navy's Naval Oceanographic Office (NavO) and the Ocean Mapping Group (OMG) over a site with lots of deployed anthropogenic objects (Hughes Clarke, 2014). The lines were run by using an EM 2040D in various swath aperture dispositions ( $\pm 72^\circ$ ,  $\pm 75^\circ$  and  $\pm 82^\circ$ ). The following configuration was set: 300 kHz, 8 knots, dual swath, three sectors and HDBF mode. In both years, WC data were retained. The test area is located at the Saanich Inlet, close to the city of Sidney, British Columbia, Canada.

The assessed targets comprise concrete cubes at the following sizes: 1-meter cube at 40 m depth, 1-meter cube at 20 m depth and 0.5 m cube at 20 m depth. The 1-meter cubes are IHO compliant targets utilized to assess the target detection performance for a Special Order survey (most stringent requirements). By turn, the 0.5-meter cube is an opportunistic test of potential Mine-like Object (MLO) detection.

The results presented in the next sections 4.1, 4.2 and 4.3 display the georeferenced sun-illuminated grayscale bathymetric DTM (25mX25m - 0.25m resolution) and the bathymetric solutions (two-dimensional across and along-track sounding profiles) around the target vicinity for the KM bottom detection method and the developed BDI algorithm in different fashions. When compressing data for the BDI solutions, 400 virtual beams were utilized (same maximum number of solutions provided by KM in high-density mode). A maximum one BDI solution per TWTT was considered.

### 4.1 1-meter cube at 40 m depth

The results for a 1-meter cube at 40 m depth ensonified at 68° of incidence angle from the 2014 dataset are presented at Fig. 14. A 72° swath angle was used.

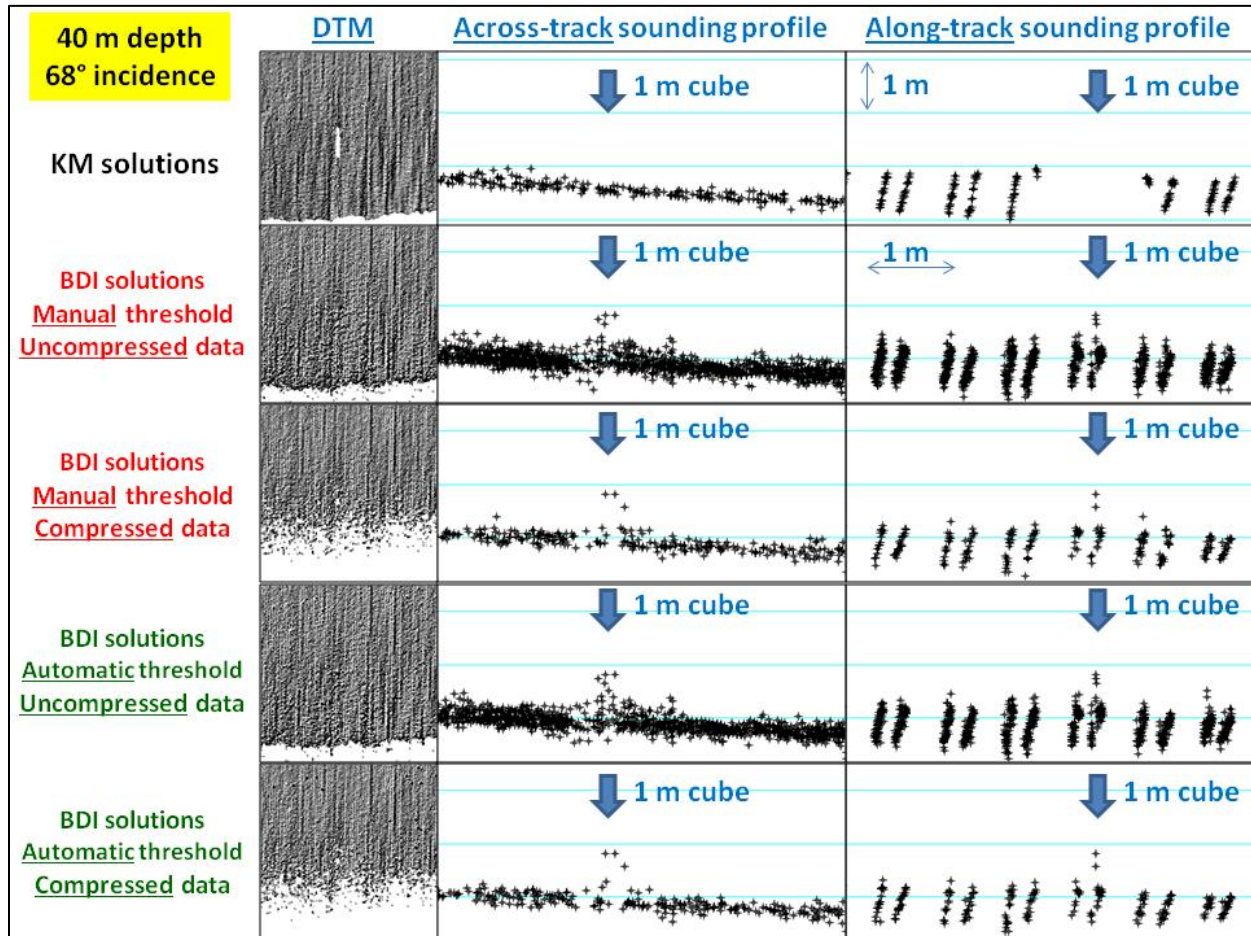


Figure 14: BDI results for 1 m cube at 40 m depth – 2014 dataset, swath width 72°

By analyzing Fig. 14, it is possible to conclude that the 1 m cube at 40 m depth seen at 68° of incidence angle was not detected by the built-in KM bottom detection algorithm. For this assessment and all others in this research, a loose target detection criterion has been adopted. It is primarily based on the visual analysis of the two-dimensional across and along-track sounding profiles. A successful detection is made if a cluster of outlying soundings in the target vicinity is observed. For that case, the real time KM solution provided only a bathymetric gap (no data) right after the target (shadow area), clearly seen in the along-track profile. Possible reasons for this unsuccessful detection are those previously discussed in section 2.2.

Concerning BDI solutions, a successful detection was made for all different fashions. Although some spurious proud soundings are noticed, the solutions over the target which are about 1 m above the surrounding seafloor clearly show its existence. The compression applied to the data somehow helps to eliminate noise, making the neighboring bottom smoother as it probably is. The target appearance when compressing the data for a maximum 400 soundings attests the BDI

ability to adequately detect the target at such low grazing angle even when limited to the maximum same number of KM solutions.

#### 4.2 1-meter cube at 20 m depth

The results for a 1-meter cube at 20 m depth ensonified at  $71^\circ$  of incidence angle from the 2013 dataset are presented at Fig. 15. An  $82^\circ$  swath angle was used.

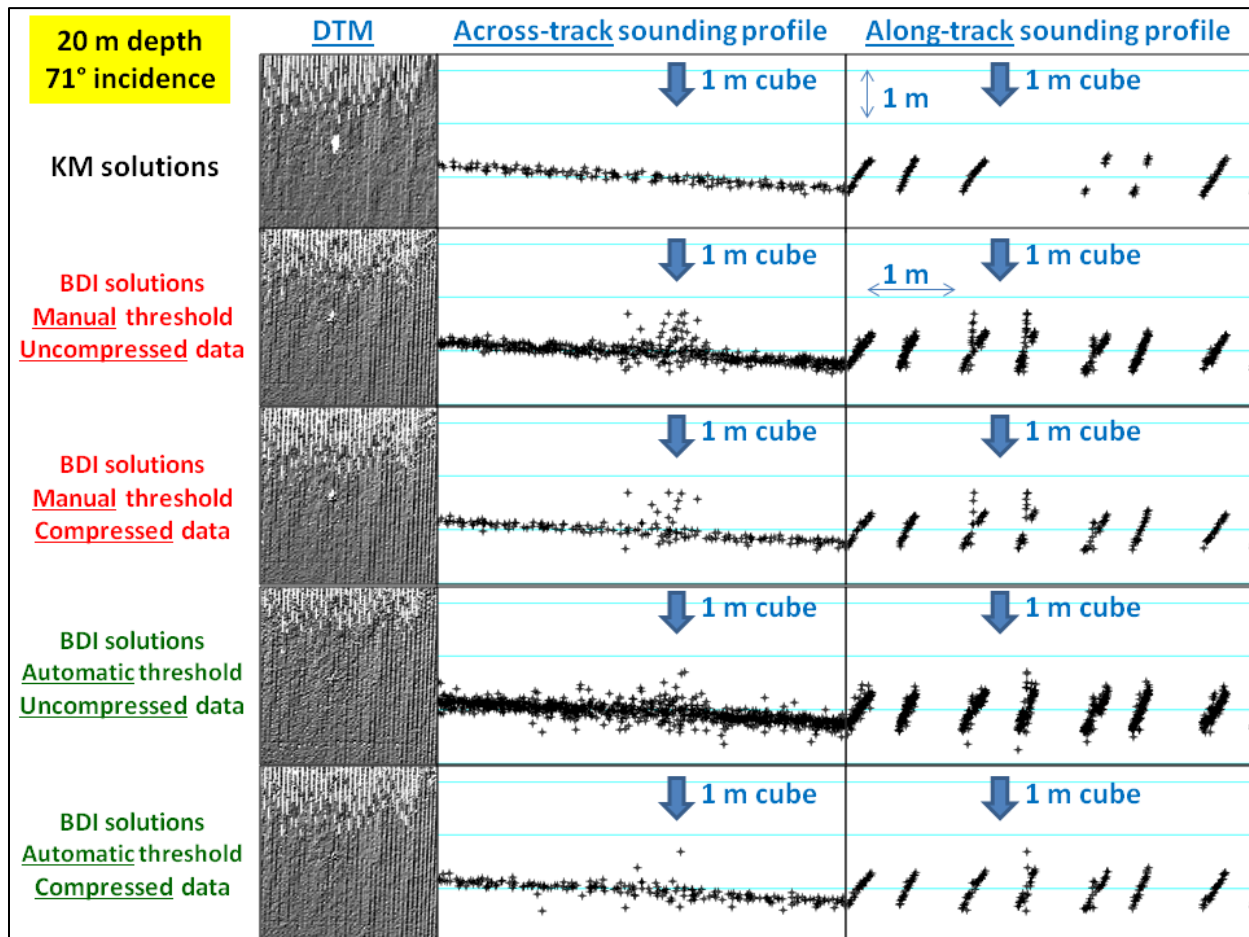


Figure 15: BDI results for 1 m cube at 20 m depth – 2013 dataset, swath width  $82^\circ$

The same analysis for the 1 m cube at 40 m depth is valid here for this 1 m cube at 20 m depth. In addition, it must be noted that the BDI user-defined threshold approach delivers better results. BDI automatic threshold yields more false solutions around target vicinity, even though the target always appears. Automatic thresholding algorithm developed for this research is a handy way to calculate the BDI solutions without the user interference or previous data analysis, although some improvements are needed for a more reliable seabed representation.

#### 4.3 0.5-meter cube at 20 m depth

The results for a 0.5-meter cube at 20 m depth ensonified at  $70^\circ$  of incidence angle from the 2014 dataset are presented at Fig. 16. A  $72^\circ$  swath angle was used.

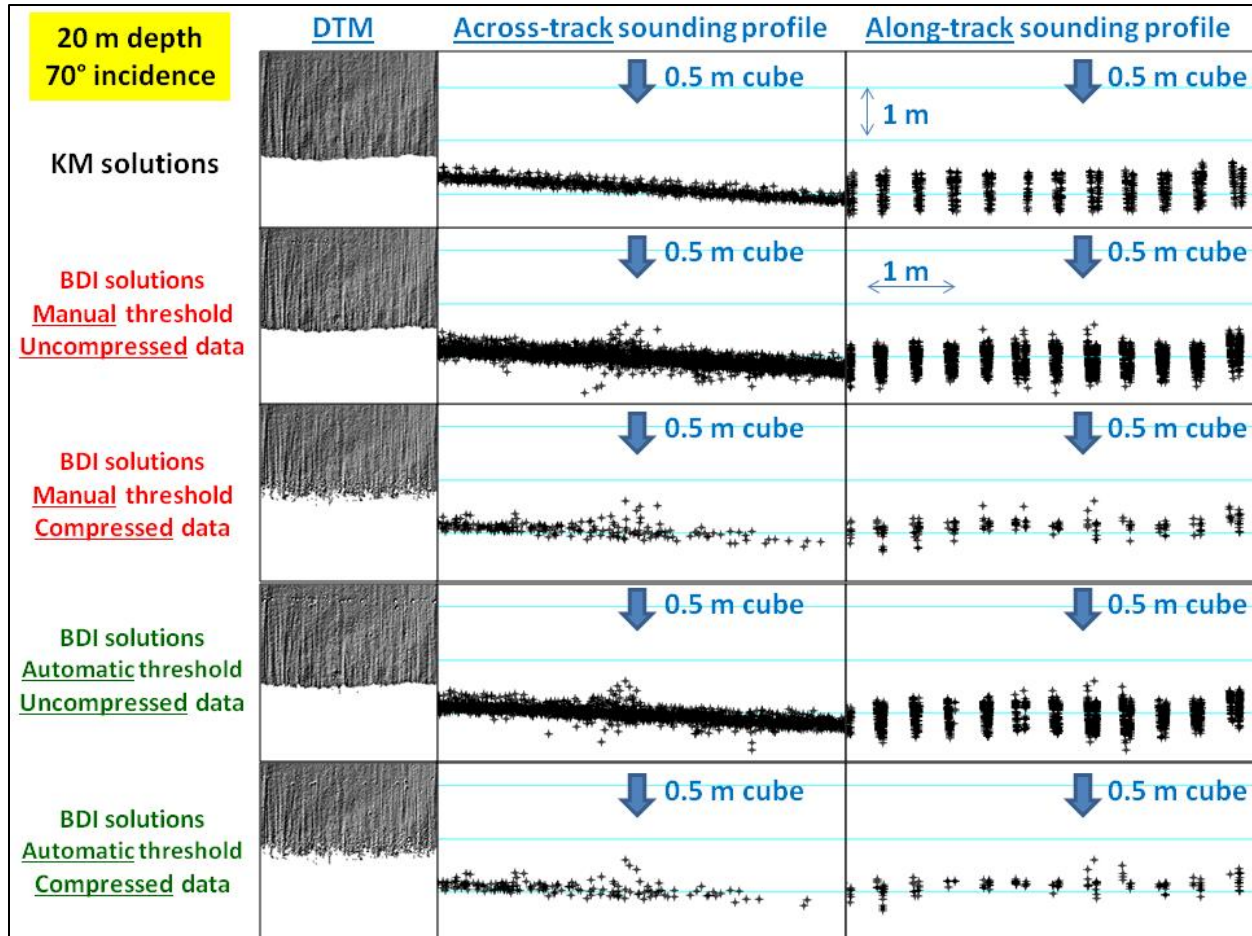


Figure 16: BDI results for 0.5 m cube at 20 m depth – 2014 dataset, swath width 72°

Again the same analysis for the 1 m cube at 40 m depth is valid here for this 0.5 m cube at 20 m depth. A data gap in the along-track profile for the KM solutions is not observed here as for the 1 m cube cases probably because of the smaller object size for the same area presentation. What is remarkable to point out is the fact that the BDI approach is able to confidently detect such small feature (0.5 m cube) at such low grazing angle (20°).

## 5. CONCLUSIONS

The well established and widespread use of WMT and Phase Detection for the multibeam bottom calculation has plenty of benefits, even though some weaknesses may appear in situations like a high aspect ratio object ensounded at low grazing angles. In this case, a reliable target detection may not be possible. For these situations, an alternative time slice by time slice BDI computation has proved to be a better approach.

The developed BDI algorithm is not a perfect solution. Some characteristics were designed to best suit the datasets used to test it. Improvements still needed include:

- the use of all samples above noise within the effective receiver main lobe beamwidth rather than only five in the parabola fitting process,

- addressing and accounting for the non-symmetric shape of the receiver main lobe beamwidth plus distortion due to TVG also in the parabola fitting process,
- refinements in both user-defined and automatic thresholding calculation to better get rid of the spurious solutions (noise) above the seafloor,
- accounting for the irregular seabed topography instead of the flat assumption when compressing the data, and
- coping with sector boundaries.

Incorporating the BDI technique into the manufacturers' bottom detection algorithms in addition to WMT and Phase Detection may be a positive approach towards a better multibeam target detection definition at low grazing angles in shallow waters. If an appropriate algorithm that smartly chooses one of the three techniques for each unique situation is made possible, certainly a more reliable seafloor representation will be accomplished.

## ACKNOWLEDGEMENTS

This work was made possible by the provision of data and operational support from the U.S. Naval Oceanographic Office (NavO). The target detection experimental layout was conceived by Rebecca Martinolich and Mel Broadus of NavO. The first author is supported by the Hydrographic Branch of the Brazilian Navy. An NSERC Discovery Grant to the second author covered logistical costs.

## REFERENCES

- Davis, P.J. (1975). Interpolation and approximation. New York: Dover Publications, Inc.
- de Moustier, C. (1993). Signal processing for swath bathymetry and concurrent seafloor acoustic imaging, in *Acoustic Signal Processing for Ocean Exploration*, J. M. F. Moura and I. M. G. Lourtie, Eds, The Netherlands: Kluwer, 329-354.
- Hammerstad, E., Pohner, F. & Bennett, J. (1991). Field testing of a new deep water multibeam echo-sounder. *Proceedings of the IEEE Oceans '91*, 2, 743-749.
- Hammerstad, E. (2008). Multibeam Echo Sounder Accuracy. Kongsberg EM Technical Note.
- Hughes Clarke, J.E. (2006). Applications of multibeam Water Column Imaging for hydrographic survey. *Hydrographic Journal*, 120(1), 3-14.
- Hughes Clarke, J.E. (2009). USNS Sumner (TAGS-61) - EM710 and EM122 Assessment. January 14<sup>th</sup>-28<sup>th</sup>, 2009, Vicinity of Saipan and Guam. Contract to U.S. Naval Oceanographic Office, via Mantech Ltd.
- Hughes Clarke, J.E. (2010). USNS Heezen (TAGS-63) - EM710 Assessment. April 16<sup>th</sup> to May 8<sup>th</sup>, 2010, Vicinity of Saipan and Guam. Contract to U.S. Naval Oceanographic Office, via Mantech Ltd.
- Hughes Clarke, J.E. (2013). HSL-16 - EM2040 dual v. single head trials. September 21<sup>st</sup> to October 21<sup>st</sup>, 2012, Orange Beach, Alabama. Contract to U.S. Naval Oceanographic Office, via Mantech Ltd.

- Hughes Clarke, J.E., Martinolich, R. & Smith, G. (2013). EM 2040 / EM 710 target detection trials: What qualifies as a successful detection? *Forum for Exchange of Mutual Multibeam Experiences (FEMME)*, Boston, USA, April 18<sup>th</sup> (presentation only).
- Hughes Clarke, J.E. (2014). HSL-16 - EM2040D Trials. Institute of Ocean Sciences, Sidney, BC, July. Contract report to U.S. Naval Oceanographic Office.
- International Hydrographic Organization (2005). Manual on Hydrography – Publication C-13 (1<sup>st</sup> Edition). International Hydrographic Bureau, Monaco.
- International Hydrographic Organization (2008). IHO Standards for Hydrographic Surveys – Special Publication No. 44 (5<sup>th</sup> Edition). International Hydrographic Bureau, Monaco.
- Kongsberg Maritime (2012). EM 2040 Multibeam Echo Sounder – Product description. Horten, Norway.
- Kongsberg Maritime (2013). EM Series Multibeam Echo Sounders – Datagram formats. Horten, Norway.
- Lurton, X. (2010). An Introduction to Underwater Acoustics – Principles and Applications (Second Edition). London: Springer / Praxis Publishing.
- Nilsen, K.E. (2011). Kongsberg EM 2040 introduction course. Horten, Norway.
- Nilsen, K.E. (2012). Kongsberg EM 2040 bottom detection course. Horten, Norway.
- Satriano, J.H., Smith, L.C. & Ambrose, J.T. (1991). Signal processing for wide swath bathymetric sonars. *Proceedings of the IEEE Oceans '91, 1*, 558-561.
- SeaBeam Instruments (2000). Multibeam sonar theory of operation (Manual), East Walpole, USA.
- van der Werf, A. (2010). Mast tracking capability of EM 3002D using Water Column Imaging. M.Sc.E. thesis, Department of Geodesy and Geomatics Engineering, University of New Brunswick, Fredericton, Canada.
- Videira Marques, C.R. (2012). Automatic mid-water target detection using multibeam water column. M.Sc.E. thesis, Department of Geodesy and Geomatics Engineering, University of New Brunswick, Fredericton, Canada.

## BIOGRAPHICAL NOTES

Douglas Pereira is a Brazilian Navy Hydrographer Officer currently pursuing his M.Sc.E. degree on Hydrography at University of New Brunswick (UNB), supervised by Dr. John E. Hughes Clarke. He has been working with hydrographic surveys since 2006, especially in the shallow waters of the Amazon River in Brazil.

John E. Hughes Clarke is the Chair in Ocean Mapping and a Professor in the Department of Geodesy and Geomatics Engineering at UNB. His prime interest lies in submarine sediment transport processes. As part of this, maximizing the information content available from integrated swath sonar systems is a major component of his research.

## CONTACTS

Douglas Luiz da Silva Pereira

Tel. +1 (506) 453-4698

Fax +1 (506) 453-4943

E-mail: [doug\\_luiz@hotmail.com](mailto:doug_luiz@hotmail.com)

John E. Hughes Clarke

Tel. +1 (506) 453-4568

Fax +1 (506) 453-4943

E-mail: [jclarke@unb.ca](mailto:jclarke@unb.ca)

Dept. Geodesy and Geomatics Engineering University of New Brunswick 15 Dineen Drive, E3B 5A3, P.O. Box 4400 Fredericton, NB CANADA
--